



ELSEVIER

Soil & Tillage Research 60 (2001) 35–42

Soil &
Tillage
Research

www.elsevier.com/locate/still

Contribution of water content and bulk density to field soil penetration resistance as measured by a combined cone penetrometer–TDR probe

Carlos M.P. Vaz^a, Luis H. Bassoi^b, Jan W. Hopmans^{c,*}

^aEmbrapa, Agricultural Instrumentation Center, P.O. Box 741, 13560-970 Sao Carlos, Brazil

^bEmbrapa, Semi-arid Center, P.O. Box 23, 56300-000, Petrolina-PE, Brazil

^cDepartment of Land, Air and Water Resources, Hydrology, University of California, 123 Veihmeyer, Davis, CA 95616, USA

Received 13 July 2000; received in revised form 4 January 2001; accepted 2 February 2001

Abstract

Soil strength as measured by cone penetrometers depends on several parameters, but it is mostly affected by the soil water content (θ) and bulk density (ρ). In order to better understand the effect of the water content and bulk density on soil strength we developed a combined penetrometer–coiled TDR probe to determine simultaneously the depth distribution of penetration resistance and water content in a soil profile. Field experiments carried out for a Yolo soil allowed the fitting of the effect of θ and ρ using a combined power–exponential equation. Using the combined cone penetrometer–TDR probe data, the fitted equation may be used to estimate soil bulk density. © 2001 Elsevier Science B.V. All rights reserved.

Keywords: Soil moisture; Soil strength; Time domain reflectometry; Cone penetrometer; Soil compaction; Soil bulk density

1. Introduction

Soil penetrability is a measure of the ease with which an object can be pushed or driven into the soil. The resistance to penetration for the cone of a penetrometer is related to the pressure required to form a spherical cavity into the soil, large enough to accommodate the cone of the penetrometer, and allowing for the frictional resistance between the cone and its surrounding soil. If the soil–cone friction is known, the point resistance of the cone may be computed from theoretical stress relations for the compression zone around the cone (Farrell and Graecen, 1966).

Soil cone penetrometers are used to characterize soil strength for assessment of soil trafficability, crop growing ability, resistance to root penetration, seedling emergence and soil compaction by machinery. Penetration resistance (PR) is influenced by soil and probe characteristics. The soil-to-probe friction is governed by probe factors such as cone angle, diameter, roughness, and rate of penetration. Soil factors influencing PR are matric potential (or water content), bulk density, soil compressibility, soil strength parameters, soil structure and others (Bradford, 1986). Although soil structure can be significant in specific conditions, in many situations it only plays a minor role (Koolen and Kuipers, 1983).

Many studies have been conducted to understand the influence of bulk density (ρ) and water content (θ)

* Corresponding author. Fax: +1-530-752-5262.
E-mail address: jwhopmans@ucdavis.edu (J.W. Hopmans).



on PR in the laboratory (Taylor and Gardner, 1963; Mirreh and Ketcheson, 1972; Ayers and Perumpral, 1982; Ayers and Bowen, 1987; Ohu et al., 1988) and field (Simmons and Cassel, 1989; Vazquez et al., 1991; Busscher et al., 1997), from which both empirical and theoretical relationships were obtained. From the many different models that have been introduced to test these relationships (polynomial, exponential, power and linear equations), Busscher et al. (1997) suggested that either the power or exponential equations are the most adequate. Using dimensional analysis techniques, Upadhyaya et al. (1982) suggested a power–exponential equation for prediction of the PR as a function of ρ and θ for a silt loam soil, but also suggested additional experimental work for its validation.

Many referenced studies lack accurate and representative data, because PR is a highly variable soil property, whereas it is usually determined from local small-scale measurements. Hence, difficulties in relating PR with other soil parameters can be attributed mostly to soil spatial variability, because available measurement techniques prevent determination of the different soil attributes (PR, θ , ρ , organic matter, texture) at the same spatial location. To improve on the measurement technique, a combined cone penetrometer–TDR moisture probe was developed by wrapping two TDR wires around the penetrometer rod (combined rod TDR) as a double helix, so that both soil water content and PR can be measured simultaneously and at approximately the same location within the soil profile (Vaz and Hopmans, 2001). The main advantage of the coiled design is that relative long travel times can be obtained, allowing accurate water content measurements for small-sized TDR probes. Although the results of the combined rod TDR were promising, some of the less satisfying results were caused by inadequate contact of the TDR coil with the surrounding soil. Moreover, the coiled rod TDR design of Vaz and Hopmans (2001) significantly increased the wall friction between the TDR coil surface around the rod and the soil, thereby likely to decrease its sensitivity to soil resistance (Koolen and Kuipers, 1983).

The objective of the present work is to determine the influence of θ and ρ on the PR for a Yolo silt clay soil from field measurements using an improved combined cone penetrometer–coiled TDR moisture

probe design that ensured adequate soil–TDR contact. PR, θ and ρ data were fitted to a combined power–exponential calibration model, as proposed by Upadhyaya et al. (1982), allowing prediction of soil bulk density from the combined probe measurements.

2. Materials and methods

2.1. TDR theory

Time domain reflectometry (TDR) is a soil moisture measurement technique (Topp et al., 1980) that is based on the velocity measurement or travel time of electromagnetic waves along a wave guide of known length inserted into the soil. The measured travel time is proportional to soil water content because of incremental changes of the bulk soil dielectric constant, as determined by the following expression:

$$T = \frac{2L\sqrt{\varepsilon}}{c} \quad (1)$$

where T (s) is the travel time, L (cm) the length of the wave guide into the soil, ε the dielectric constant of the soil around the wave guide and c (cm s^{-1}) the speed of light.

Routinely, an experimental relation between a gravimetrically measured water content and the bulk soil dielectric constant as measured with TDR is determined to yield a calibration curve that is valid for a wide water content range. The calibration procedure may use the polynomial fitting approach as suggested by Topp et al. (1980) or apply physical based models such as the mixing models of Dobson et al. (1985), Dirksen and Dasberg (1993) and Dasberg and Hopmans (1992).

2.2. Probe description

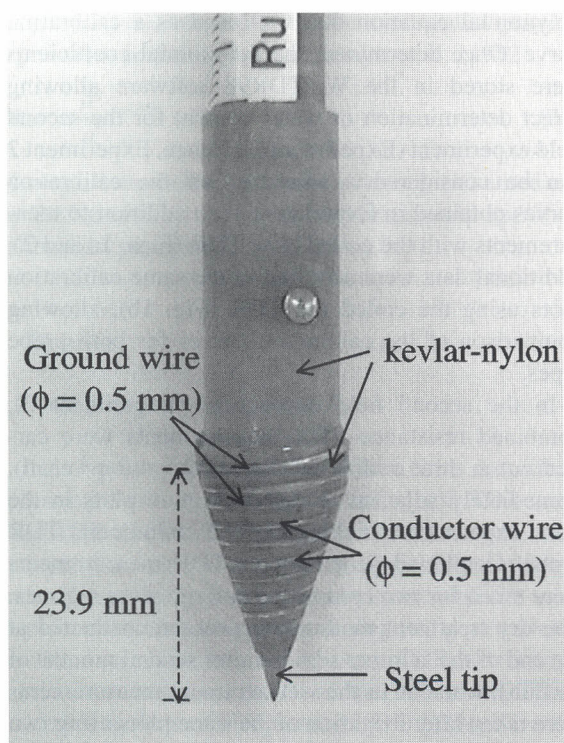
In the earlier coiled TDR probe design of Vaz and Hopmans (2001), two parallel copper wires were coiled around a PVC core along the penetrometer steel rod, above the cone of the penetrometer (coiled rod TDR). Although the coiled rod TDR was successfully tested and calibrated in the laboratory and field (Vaz and Hopmans, 2001), additional field measurements indicated that at high soil water content the probe–soil contact was poor, thereby significantly

affecting dielectric constant measurements. The penetrometer used is an impact-loading or hammer penetrometer, and was selected because of its simplicity and ease of construction. A detailed description of the penetrometer used can be found in Vaz and Hopmans (2001).

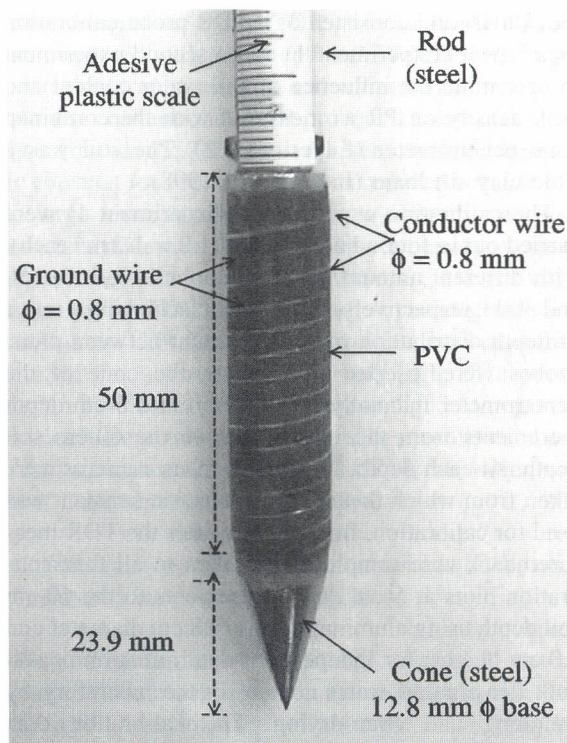
The presented probe design in this study uses two parallel steel wires (conductor and ground) wrapped around the insulation-covered cone of the penetrometer (coiled cone TDR), thereby improving contact between the TDR coil and the surrounding bulk soil. A photo with a short description of the various components of both the coiled cone TDR and coiled rod TDR probe assembled with the penetrometer rod is shown in Fig. 1a and b, respectively. In addition to the position of the coiled TDR wires, the field-tested coiled cone TDR probe in this study differs from the coiled rod TDR (Vaz and Hopmans, 2001) in size, diameter and length of the TDR wires. The coiled cone TDR is made of two parallel steel wires, each

0.5 mm diameter and 15 cm long, coiled along a Kevlar-Nylon (hard plastic material) cone, with a 2 mm separation between the wires as shown in Fig. 2. The cone has a base diameter of 12.8 mm and is 23.9 mm long, whereas the steel tip is bare without nylon material. Cone size satisfies the American Society of Agricultural Engineers Standards (ASAE, 1994).

Wires are soldered with the conductor and ground of a 50 Ω coaxial cable internally to the penetrometer steel tube (Fig. 2). The 2.5-m long coaxial cable is guided through the penetrometer hollow-probing rod and connected to a Tektronix 1502C cable tester for bulk soil dielectric constant measurements. A laptop computer was connected to the cable tester to determine the soil bulk dielectric constant. Water content was estimated from the probe-specific calibration procedure, as presented later, using the WinTDR98 software available at <http://psb.usu.edu/wintdr98/> (Or et al., 1998).



(a)



(b)

Fig. 1. Photographs of (a) the coiled cone TDR and (b) the coiled rod TDR of Vaz and Hopmans (2001).

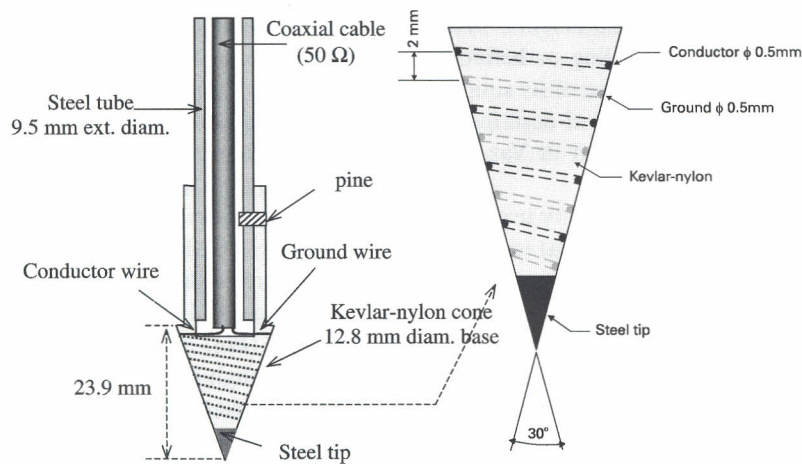


Fig. 2. Schematic drawing of coiled cone TDR probe of the improved combined penetrometer–cone TDR probe design.

2.3. Field experiment

The experiments were conducted at the Campbell Tract experimental field of the University of California, Davis, and consisted of a TDR probe calibration experiment (Experiment 1) and a second experiment to determine the influence of soil water content and bulk density on PR as measured with the combined cone penetrometer (Experiment 2). The soil was a Yolo clay silt loam (Inoue et al., 1998).

The calibration experiments (Experiment 1) were carried out in four adjacent plots ($1.2 \times 1.2 \text{ m}^2$ each), with different amount of water applied (0, 100, 150 and 300 l, respectively) to each plot, achieving a range of depth distribution of water content between plots. Probes were inserted by pushing the cone of the penetrometer manually into the soil at 2.5-cm depth increments from the soil surface to the 60-cm soil depth. At each depth, three TDR measurements were taken from which the average dielectric constant was used for calibration. Immediately after the TDR measurements, core samples were taken in all four calibration plots at 5-cm depth increments to the 60-cm soil depth using aluminum rings (4.8 cm diameter and 5.0 cm height) for independent determination of soil bulk density and water content in the laboratory by weighing and oven-drying. The calibration data (dielectric constant versus water content) were obtained by combining two successive 2.5-cm TDR measurements to yield 5-cm depth-averaged bulk soil

dielectric values, corresponding with the 5-cm depth intervals of gravimetric soil water content and density values.

The calibration data were fitted to a third-order polynomial equation that was used as a calibration curve. Once determined, the polynomial coefficients were stored in the WinTDR98 software allowing direct determination of water content for the second field experiment (Experiment 2). Hence, Experiment 2 can be considered a validation of the calibration curves obtained in Experiment 1. In addition to measurements with the coiled cone TDR (Figs. 1a and 2), additional data were acquired in the same calibration plots using the coiled rod TDR (Fig. 1b), allowing comparison of the calibration curves for both probe types.

In the second field experiment (Experiment 2), combined resistance–TDR measurements were carried out in three additional plots ($1.2 \times 1.2 \text{ m}^2$ each), immediately adjacent to the calibration plots in the same experimental field, using the coiled cone TDR probe. Combined penetrometer–TDR measurements were taken for two contrasting soil moisture regimes. The dry treatment measurements were conducted at the end of the summer season (after several months of no rain), whereas in the wet treatment measurements were taken after irrigation of the same plots using two 26-mm water applications. Soil PR was computed from the depth of penetration of the cone penetrometer after each impact (Vaz and Hopmans, 2001), based on

energy conservation principles, yielding (Vaz and Hopmans, 2001)

$$PR = 0.40624 + \frac{0.09135}{x} \quad (2)$$

where PR (MPa) is the penetration resistance and x (m) the penetration distance. The numerical values in Eq. (2) vary with the mass of the hammer and penetrometer, cone geometry, and hammer drop height.

TDR measurements were carried out immediately after recording the depth of penetration for each impact. Depth distribution of volumetric water content was determined from the calibration curve obtained in the first calibration experiment. In addition, depth-averaged bulk density values corresponding with the measuring depths (each 5 cm from 0 to 60 cm depth), were determined from the samples collected in the calibration plots of Experiment 1. The corresponding 5-cm depth-averaged PR (MPa) and water content (θ , $\text{cm}^3 \text{cm}^{-3}$) measured at the three experimental plots of Experiment 2 using the combined penetrometer–cone TDR probe for the two water regimes and bulk density (ρ , g cm^{-3}) data were fitted to the exponential–power expression, proposed by Upadhyaya et al. (1982)

$$PR = a \frac{\rho^n}{\rho_s} e^{-b\theta} \quad (3)$$

where ρ_s denotes the soil particle density (assumed to be 2.65 g cm^{-3}), and a , n , and b are soil-specific calibration parameters.

3. Results

3.1. Calibration (Experiment 1)

Fig. 3 presents the calibration data with the fitted polynomial curves for both the coiled rod TDR and cone TDR probes. Differences of dielectric constants between two probes are mostly attributed to differences in probe geometry, probe–soil contact, soil displacement and compaction during soil penetration. As the data show, the coiled cone TDR was more sensitive to water content than the coiled rod TDR presented by Vaz and Hopmans (2001) for high water content values, most likely so because of the improved probe–soil contact of the coiled cone TDR. As pointed out in Vaz and Hopmans (2001), air gaps are likely to

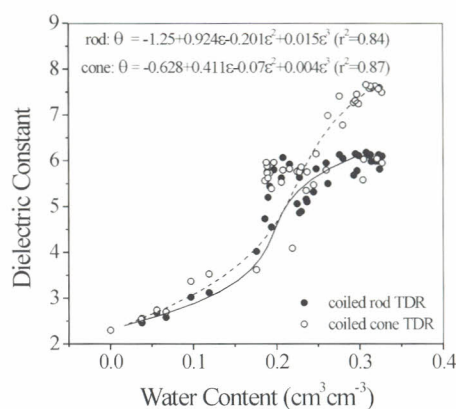


Fig. 3. Calibration curves for the coiled cone (open circles) and rod (solid dots) TDR of Experiment 1.

occur in some soil conditions for the coiled rod TDR, thereby reducing the measured travel time and bulk dielectric constant. In contrast the cone design ensures excellent soil contact with the TDR probes during probe insertion.

As one would expect, the bulk dielectric constant, as measured with the coiled TDR probes is much lower than measured with a conventional TDR probe (Topp et al., 1980), at equal bulk soil water content values. For most conventional TDR probes, the soil completely surrounds the TDR rods, whereas the bulk dielectric constant for the coiled TDR is reduced because of the large contribution of the low dielectric of the insulator material (PVC, nylon or epoxy resin) between the coiled wires. Nevertheless, the sensitivity of the coiled TDR is very good, especially for the coiled cone TDR, because travel times measured for the 15 cm long wires are sufficiently high. Data were fitted to third-order polynomials (see Fig. 3 for regression coefficient values) that were subsequently used as calibration curves in the WinTDR98 software for direct determination of soil water content.

3.2. Influence of soil water content and bulk density on penetration resistance (Experiment 2)

Depth distribution of PR (a) and volumetric water content (b) as determined from measurements with the combined penetrometer–coiled cone TDR probe (Fig. 1a) are presented in Fig. 4. Averages of the three plots are presented as “dry” (before irrigation) and “wet” (after irrigation). The lack of water content data

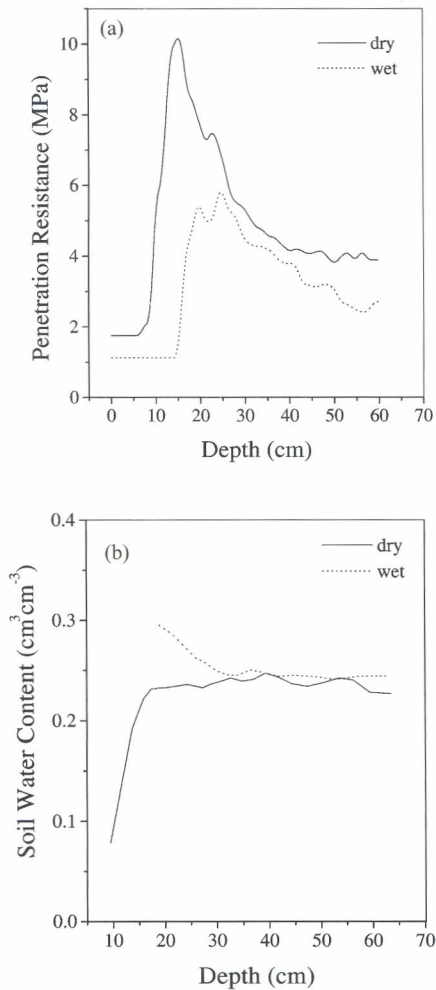


Fig. 4. Average field-measured depth distribution of PR (a) and θ (b) of the dry (solid line) and wet (dotted line) treatments, using the combined penetrometer–coiled cone TDR probe.

in Fig. 4b for the wet treatment was caused by the soil surface's low resistance, resulting in a depth of penetration (x) of about 18 cm after only the first hammer drop. PR data clearly show a decrease of the PR after irrigation as a result of the increasing water content (Fig. 4b), with a maximum resistance at the 15–25 cm soil depth for both the dry and wet treatments, likely caused by an increased soil bulk density at that depth interval. This soil density maximum at the 15–25 cm soil depth was confirmed by independently collected bulk soil density samples used for the calibration curve of Experiment 1. These measured density data

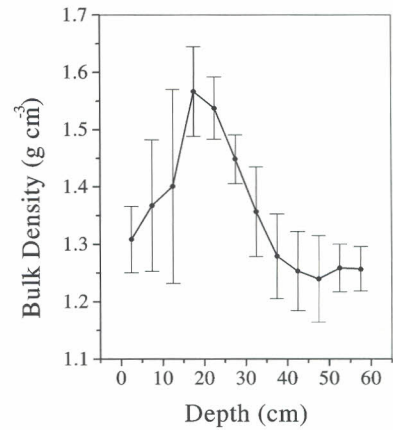


Fig. 5. In situ depth distribution of dry bulk density of the calibration plots of Experiment 1. Bars indicate standard deviation as calculated from four cores per sampling depth.

are presented in Fig. 5, with the bars designating the standard deviation of four core samples for each depth, as obtained from the calibration plot sampling.

Comparison of the coiled cone TDR with the rod cone TDR (results not presented) showed that the PR of the coiled rod TDR was much higher due to an additional friction effect along the coiled rod TDR wall during penetration (Vaz and Hopmans, 2001). The increased wall friction of the rod TDR makes the penetrometer less suitable as PR may be dominated by friction effects, whereas the measurement objective is to evaluate soil effects. Also, the coiled rod TDR water content measurements (results not presented) were more scattered, likely due to poor soil–TDR contact at high water content values.

The combined penetrometer–cone TDR data for the three plots are averaged and presented in Fig. 6 for both the dry and wet soil treatments. PR is presented as a function of θ , with different symbols indicating ranges in magnitude of depth-averaged dry bulk soil density (ρ). As expected, there is a tendency of PR to increase as ρ increases at equal θ values. Moreover, the fitted curves demonstrate the intuitive-correct results that (1) the bulk density effect on PR decreases as the water content increases and (2) PR increases exponentially with decreasing water content. Data for the 0–5 and 5–10 cm were not included in Fig. 6, because the PR of the tilled soil surface was too low, irrespective of its water content. Using the model-fitting software of Wraith and Or (1998), the PR, θ ,

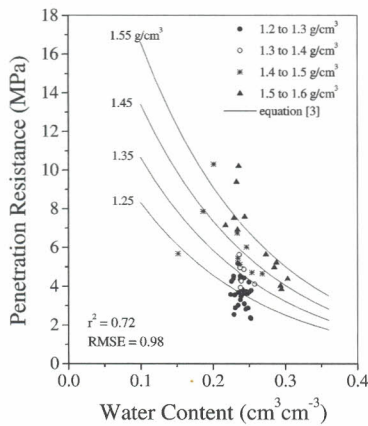


Fig. 6. Functional relationship between PR and volumetric water content (θ), for different dry bulk soil density (ρ) ranges for Experiment 2. Symbols denote measured data, and solid lines represent fitted curves using Eq. (3).

and ρ data in Fig. 6 were fitted to Eq. (3), yielding soil-specific parameter values of $a = 170.15$, $n = 3.22$, and $b = 5.99$, resulting in a R^2 -value of 0.72 and a root mean squared error, RMSE, of 0.98 MPa. The fitted curves are also presented in Fig. 6, using ρ -values of 1.25, 1.35, 1.45 and 1.55 g cm^{-3} . We conclude that Eq. (3) of Upadhyaya et al. (1982) described the experimental data fairly well within the water content range of 0.15–0.30 $\text{cm}^3 \text{cm}^{-3}$. Scattering of data presented in Fig. 6 was caused by a combination of factors such as the relatively narrow range of water content; different sampling locations of combined probe (Experiment 2) and gravimetric sampling (Experiment 1), and the expected variation of PR within each ρ -class since soil samples varied in bulk density within each density class.

To demonstrate the sensitivity of Eq. (3) to soil bulk density, we used the measured PR and θ data of Fig. 6 to estimate the dry bulk density of the respective soil layers of all three plots, using Eq. (3) with its fitted parameter values. The resulting mean and standard deviation of ρ are compared with the respective measured values (from Experiment 1) in Fig. 7. Estimated and measured soil density data from the soil profile were very well correlated, with a correlation coefficient of 0.98. However, verification of Eq. (3) to estimate field soil bulk density in a large field experiment is still needed.

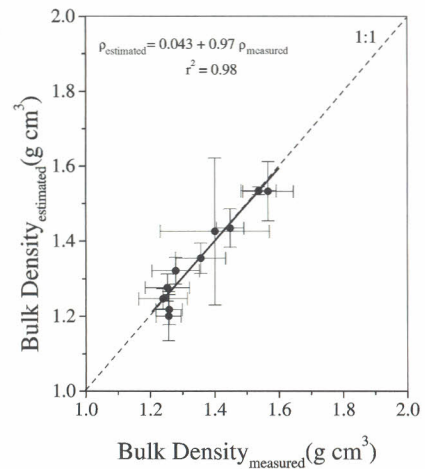


Fig. 7. Comparison of measured (horizontal axis, Experiment 1) with predicted (vertical axis) dry bulk density values, using fitted regression equation (3).

4. Conclusion

It has been shown that coiled wires can be combined with the cone penetrometer so that both soil resistance and corresponding soil water content can be measured to assess the influence of soil density and water content on soil resistance. The unique combined penetrometer–TDR probe, with paired wires coiled around the cone, allows for simultaneous measurement of both soil resistance and water content, within the same soil volume at the same spatial location, thereby preventing complications that can arise because of soil heterogeneity. We have demonstrated that the TDR component of the combined probe is sufficiently sensitive to water content changes, even though the bulk dielectric value of the measured domain is significant less than for bulk soil alone. However, the size and geometry of the measured soil domain still needs to be investigated, and will depend on the exact configuration of the coiled wires within the cone. Moreover, we have demonstrated the validity of the exponential–power function to relate measured PR (from penetrometer measurements) to dry soil bulk density (independently measured) and water content (as estimated from the combined cone penetrometer–TDR probe measurements).

The increased sensitivity of the presented combined probe, as compared with an earlier design was

achieved by improved soil–TDR contact. Moreover, the inclusion of the TDR within the cone decreased the friction effect on the PR measurement. In an ongoing project, the effectiveness of the presented design to evaluate the influence of water content and soil density on soil strength will be further investigated from high spatial resolution field measurements.

Acknowledgements

We wish to thank FAPESP (98/04740-7), Embrapa and University of California Davis for the financial support and David Page, Mike Mata and Jim MacIntyre for their assistance in the construction of the coiled cone TDR probe and in the field experiment.

References

- ASAE, 1994. ASAE standards engineering practices data (soil cone penetrometer, S313.2), St. Joseph.
- Ayers, P.D., Bowen, H.D., 1987. Predicting soil density using cone penetration resistance and moisture profile. *ASAE Trans.* 30, 1331–1336.
- Ayers, P.D., Perumpral, J.V., 1982. Moisture and density effects on cone index. *ASAE Trans.* 25 (5), 1169–1172.
- Bradford, J.M., 1986. Penetrability. In: Klute, A. (Ed.), *Methods of Soil Analysis. Part 1. Physical and Mineralogical Methods*, 2nd Edition, Monograph Number 9. American Society of Agronomy, Madison, WI.
- Busscher, W.J., Bauer, P.J., Camp, C.R., Sojka, R.E., 1997. Correction of cone index for soil water content differences in a coastal plain soil. *Soil Till. Res.* 43, 205–217.
- Dasberg, S., Hopmans, J.W., 1992. Time domain reflectometry calibration for uniformly and nonuniformly wetted sandy and clayey loam soils. *Soil Sci. Soc. Am. J.* 56, 1341–1345.
- Dirksen, C., Dasberg, S., 1993. Improved calibration of time domain reflectometry soil water content measurements. *Soil Sci. Soc. Amer. J.* 57, 660–667.
- Dobson, M.C., Ulaby, F.T., Hallikainen, M.T., El-Rayes, M.A., 1985. Microwave dielectric behavior of wet soil: II Dielectric mixing models. *IEEE Trans. Geosci. Remote Sensing* GE 23, 35–46.
- Farrell, D.A., Graecen, E.L., 1966. Resistance to penetration of fine probes in compressible soils. *Aust. J. Soil Res.* 4, 1–17.
- Inoue, M., Simunek, J., Hopmans, J.W., Clausnitzer, V., 1998. In-situ estimation of soil hydraulic properties using a multistep soil-water extraction technique. *Water Resour. Res.* 34 (5), 1035–1050.
- Koolen, A.J., Kuipers, H., 1983. *Agricultural Soil Mechanics*. Springer, Berlin.
- Mirreh, H.F., Ketcheson, J.W., 1972. Influence of bulk density and matric pressure to soil resistance to penetration. *Can. J. Soil Sci.* 52, 477–483.
- Ohu, J.O., Raghavan, G.S.V., McKyes, E., 1988. Cone index prediction of compacted soils. *ASAE Trans.* 31 (2), 306–310.
- Or, D., Bisher, B., Hubscher, R.A., Wraith, J., 1998. WinTDR98 software V4.0. User Guide. On-line Manual-format PDF, Plant Soil & Biometeorology, Utah State University, 76 pp.
- Simmons, F.W., Cassel, D.K., 1989. Cone index and soil physical properties relationships on sloping paleudult complex. *Soil Sci.* 147, 40–46.
- Taylor, H.M., Gardner, H.R., 1963. Penetration of cotton seedling taproot as influenced by bulk density, moisture content, and strength of the soil. *Soil Sci.* 96, 153–156.
- Topp, G.C., Davis, J.L., Annan, A.P., 1980. Electromagnetic determination of soil water content: measurements in coaxial transmission lines. *Water Resour. Res.* 16, 574–582.
- Upadhyaya, S.K., Kemble, L.J., Collins, N.E., 1982. Cone index prediction equations for Delaware soils. *ASAE Paper* 82, 1452–1456.
- Vaz, C.M.P., Hopmans, J.W., 2001. Simultaneous measurement of soil strength and water content with a combined penetrometer–moisture probe. *Soil Sci. Soc. Am. J.* 65 (1), 4–12.
- Vazquez, L., Myhre, D.L., Hanlon, E.A., Gallaher, R.N., 1991. Soil penetrometer resistance and bulk density relationships after long-term no tillage. *Commun. Soil Plant Anal.* 22, 2101–2117.
- Wraith, J.M., Or, D., 1998. Nonlinear parameter estimation using spreadsheet software. *J. Nat. Resour. Life Sci. Educ.* 27, 13–19.